



Direct Detection of Manganese Ions in Organic Electrolyte by UV-vis Spectroscopy

L. Zhao,^{1,2} E. Chénard,³ Ö. Ö. Çapraz,^{1,2,4} N. R. Sottos,^{1,2} and S. R. White^{1,2,4,z}

¹Department of Material Science and Engineering, University of Illinois at Urbana-Champaign, Urbana, Illinois 61801, USA

²Beckman Institute of Science and Technology, University of Illinois at Urbana-Champaign, Urbana, Illinois 61801, USA

³PCAS CANADA, St-Jean-sur-Richelieu, Québec J3B8J8, Canada

⁴Aerospace Engineering, University of Illinois at Urbana-Champaign, Urbana, Illinois 61801, USA

Lithium manganese oxide cathodes used in Li-ion batteries suffer from manganese dissolution and capacity fade. We present a new technique for directly measuring the manganese ion (Mn^{2+}) concentration in a typical Li-ion carbonate electrolyte using 4-(2-pyridylazo) resorcinol (PAR) as a UV-vis probe. Chelation between PAR and Mn^{2+} ion induces a characteristic absorption peak where the peak intensity corresponds to Mn^{2+} ion concentration in the electrolyte. Electrochemical stability of the probe is verified by performing potential hold and cyclic voltammetry. The in situ characterization of Mn dissolution in a customized battery cell is performed during cyclic voltammetry.

© 2018 The Electrochemical Society. [DOI: [10.1149/2.1111802jes](https://doi.org/10.1149/2.1111802jes)]

Manuscript submitted November 7, 2017; revised manuscript received January 15, 2018. Published January 27, 2018. This was Paper 148 presented at the National Harbor, Maryland Meeting of the Society, October 1–5, 2017.

Li-ion batteries have been primarily used in portable electronics for more than two decades. Recent developments in electronic vehicles demand higher energy capacity and faster charge-discharge rates. Lithium manganese oxide ($LiMn_2O_4$, LMO) is a promising cathode material for the next generation of lithium ion batteries due to its high capacity, low cost, and low toxicity.¹ However, LMO suffers from Mn^{2+} ion dissolution that results in rapid capacity degradation in Li-ion batteries.^{2–5} Manganese dissolution has been investigated at elevated temperature,² overdischarge⁶ and high electrolyte acidity conditions.⁷ Mn^{2+} ion concentration in electrolytes has been measured primarily using ex situ techniques such as atomic absorption spectroscopy (AAS),⁸ chemical titration,⁹ differential pulse voltammetry² and inductively coupled plasma mass spectrometry (ICP-MS).¹⁰ Although ex situ techniques reveal some factors affecting manganese dissolution, they do not provide sufficient information to understand the detailed manganese dissolution mechanisms occurring.¹¹

The in situ detection of Mn^{2+} ions in electrolytes has been attempted previously.^{12,13} Terada et al. reported an increase in manganese ion concentration in the electrolyte with electrochemical cycle number by in situ sampling of the electrolyte with a capillary extraction tube and subsequent ex situ total reflection X-ray fluorescence (TXRF) analysis.¹² However, the technique can only measure manganese ion concentration over a relatively lengthy period of time in each cycle due to a limited sampling rate. Wang et al. used a rotating ring disk electrode (RRDE) to investigate the dissolution of manganese by collecting dissolved Mn^{2+} ions on a ring electrode and measuring the ring current.¹³ However, a high scan rate (100 mV/s) is required for this technique, and cyclic voltammetry at this scan rate cannot resolve any detailed understanding of the lithium intercalation process. A real-time, non-destructive manganese detection method with high resolution is needed to understand the dissolution mechanism of Mn^{2+} during charging and discharging of Li-ion batteries.

UV-vis spectroscopy is a potential technique for quantitatively determining the concentration of a certain chemical species (e.g. Mn^{2+}) by its optical absorption spectrum. Detection of Mn^{2+} ions in a battery electrolyte via UV-vis spectroscopy requires a chemical probe that will combine with a Mn^{2+} ion and alter the absorption spectrum. The probe must be stable in the electrochemical environment experienced by Li-ion batteries.¹⁴ Furthermore, the probe must be selective and capable of distinguishing Mn^{2+} ions from other ions present (e.g. Li^+) in the electrolyte.⁹

The chemical probe 4-(2-pyridylazo) resorcinol (PAR) has been reported to form a stable complex with transition metal ions in neu-

tral to basic aqueous solutions.¹⁵ Its excellent selectivity of transition elements enables PAR to selectively detect Mn^{2+} ions even in the presence of concentrated Li^+ ions within the electrolyte. However, an organic base is required as a proton absorber¹⁶ in order to activate the PAR within the electrolyte. Here, we present a new technique for the in situ detection of Mn^{2+} ion concentration in Li-ion battery electrolyte by using PAR as a Mn-ion indicator and employing UV-vis spectroscopy. The technique is potentially applicable for operando detection of Mn^{2+} ions during charging/discharging of Li-ion batteries.

Experimental

Electrolyte solvent for all electrochemical testing consists of 1 mol/L $LiPF_6$ (98%, Sigma Aldrich) in ethylene carbonate (EC, Anhydrous, 99%, Sigma Aldrich) and dimethyl carbonate (DMC, Anhydrous, >99%, Sigma Aldrich) 1:1 by volume. 3 mL vials of electrolyte containing 31 $\mu\text{mol/L}$ 4-(2-pyridylazo) resorcinol (PAR, 96%, Sigma Aldrich), 2.3 mmol/L proton sponge (PS, 1,8-Bis(dimethylamino)naphthalene, Sigma Aldrich) and different concentrations (0~20 $\mu\text{mol/L}$) of $Mn(acac)_2$ (Sigma Aldrich) were prepared in Ar glove box. The electrolytes were then analyzed by UV-vis spectrometer (Shimadzu UV-2401PC).

The electrochemical stability of PAR and PS were tested in a 20-mL beaker cell with a Pt wire as the cathode and Li foil (Alfa Aesar) as the anode. The electrodes were separated by 1 cm and placed within a glass beaker to which was added 7.5 mL of the electrolyte containing PAR/PS and $Mn(acac)_2$. Either a constant voltage of 4.5 V for 1.5 hours or a constant voltage rate of 1 mV/s from 3.5 V to 4.5 V were applied with a battery cycler (Arbin, BT 2000).

For in situ detection, an alternative organic phosphazene base (BTPP, tert-butylimino-tri(pyrrolidino)phosphorane, Sigma Aldrich) was chosen for better long-term stability. The customized cell for electrolyte spectroscopic analysis was modified from the design reported by Jones et al.,¹⁷ and is shown in Figure 1. A 2-mm diameter aperture was included at the back of cell, located between the LMO cathode and the Li metal anode, and sealed with a quartz window. The cell was aligned such that the incident light penetrates through the aperture and is received by the UV-vis detector through the front window. LMO cathode was prepared by casting a slurry consisting of $LiMn_2O_4$ (electrochemical grade, Sigma Aldrich), Super P carbon black, carboxymethyl cellulose sodium salt (Sigma Aldrich), and DI water in a 8:1:1:50 weight ratio. The slurry mixture was homogenized at 8000 rpm for 1 hour, casted with a doctor blade set at 15 μm onto 15 μm thick Al foil blasted with grit 600 sand paper, and dried in

^zE-mail: swhite@illinois.edu

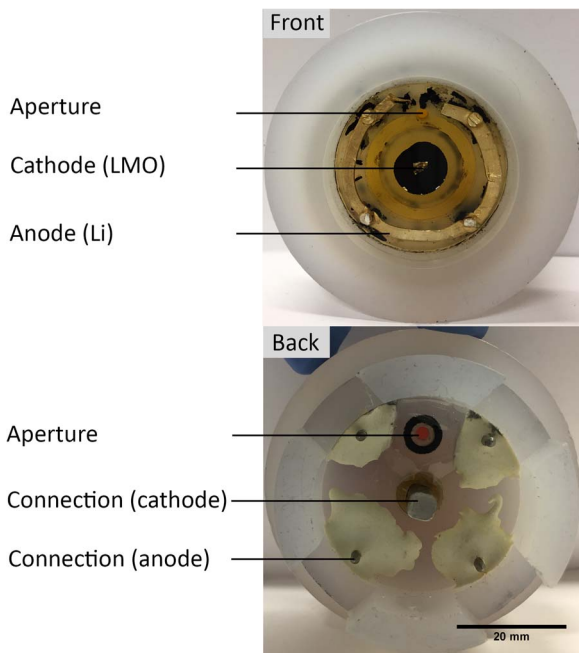


Figure 1. Custom battery cell for in situ electrolyte spectroscopic analysis during cyclic voltammetry.

ambient conditions overnight. The dried cathode film was then cut into a 12.7 mm diameter disk and spot-welded onto the current collector of the customized cell. The cell was then cycled at $\pm 50 \mu\text{V}/\text{s}$ between 3.5 V and 4.5 V. The UV-vis absorption spectrum of the electrolyte was recorded every minute during electrochemical cycling.

Results and Discussion

Mn^{2+} ion concentration in the electrolyte was detected using PAR as a UV-vis indicator and PS as an activator. The role of the PS is to deprotonate the PAR molecule and enable its chelation with Mn^{2+} ions. The stability constant of the complex between the deprotonated PAR and a Mn^{2+} ion is $\sim 10^6$ times higher than the protonated one in aqueous conditions.¹⁸ In a carbonate solvent, as is typical for Li-ion batteries, the protonated PAR cannot react with Mn^{2+} without the presence of the PS. Figures 2a and 2b show the optical image and the UV-vis spectra of electrolytes with PAR and PS at different Mn^{2+} ion concentrations obtained by adding different concentrations of $\text{Mn}(\text{acac})_2$. In the absence of Mn^{2+} ions, the electrolyte exhibits a yellow-orange color and its spectrum shows an absorption peak at 490 nm wavelength. As the Mn^{2+} ion concentration increases, a new absorption peak at 534 nm emerges and the electrolyte color becomes bright red.

The electrolyte spectrum with only PAR and PS present ($\text{Mn}^{2+} = 0 \mu\text{mol/L}$) is subtracted from raw spectra in order to highlight the characteristic peak of the PAR- Mn^{2+} complex at 534 nm in Figure 2c. By extracting the characteristic peak intensity with respect to Mn^{2+} ion concentration, a calibration curve is generated in Figure 2d. At concentrations below $16 \mu\text{mol/L}$, the peak intensity is linear with respect to Mn^{2+} ion concentration, as is expected from the Beer-Lamber Law, with a correlation coefficient 0.997. At Mn^{2+} ion concentrations above $16 \mu\text{mol/L}$, the absorption peak intensity saturates and begins to deviate from linearity. Thus, quantifying the concentration of Mn^{2+} ions is possible via UV-vis spectroscopy up to certain concentration range. Increasing the PAR/PS concentration within the electrolyte can expand the detectable range as well.

Electrochemical stability of the PAR-PS probe was examined by applying external voltage. Platinum and lithium electrodes were used as the cathode and anode respectively of a battery cell in order to avoid introducing any manganese during the electrochemical test. Mn^{2+} ions

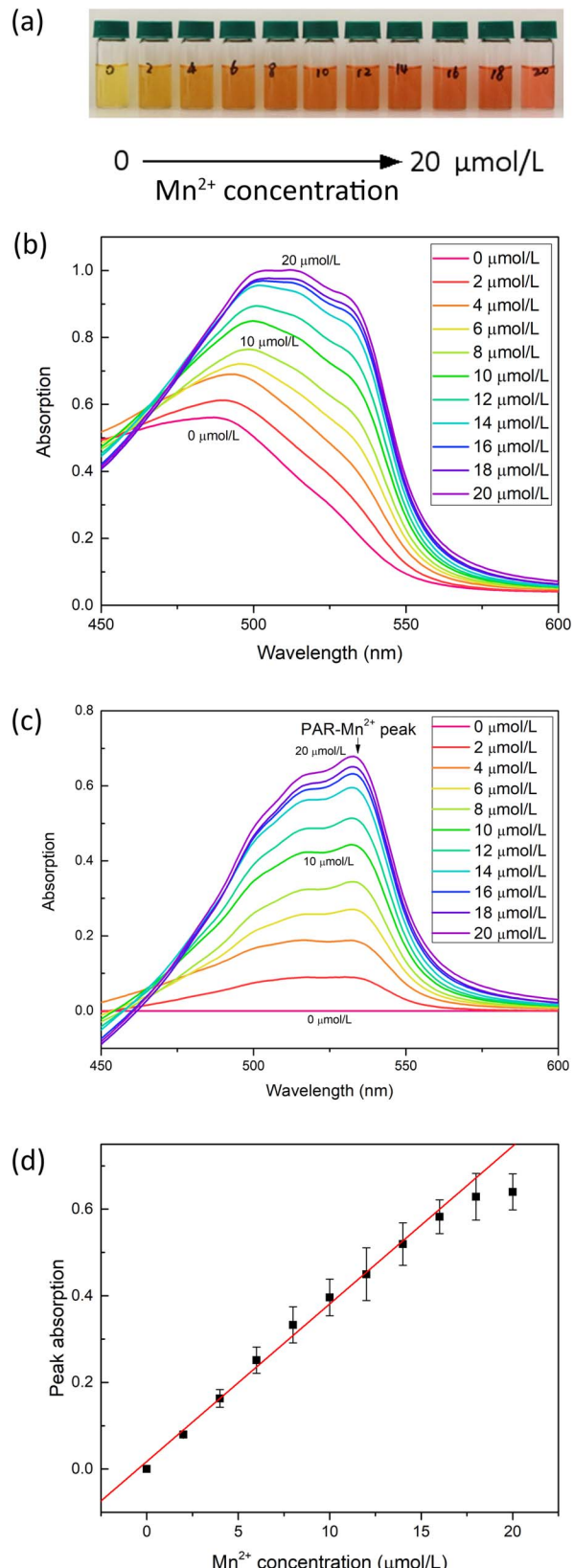


Figure 2. The detection of Mn^{2+} ion concentration in Li-ion battery electrolyte with a UV-vis probe. (a) Optical image of electrolytes with the probe PAR/PS at different Mn^{2+} ion concentrations. The numbers on vials correspond to Mn^{2+} ion concentration in $\mu\text{mol/L}$. (b) Raw UV-vis spectra of electrolytes in (a). (c) Spectra after background subtraction of the $\text{Mn}^{2+} = 0 \mu\text{mol/L}$ case. (d) Calibration curve of peak intensity at 534 nm from (c) vs. Mn^{2+} concentration.

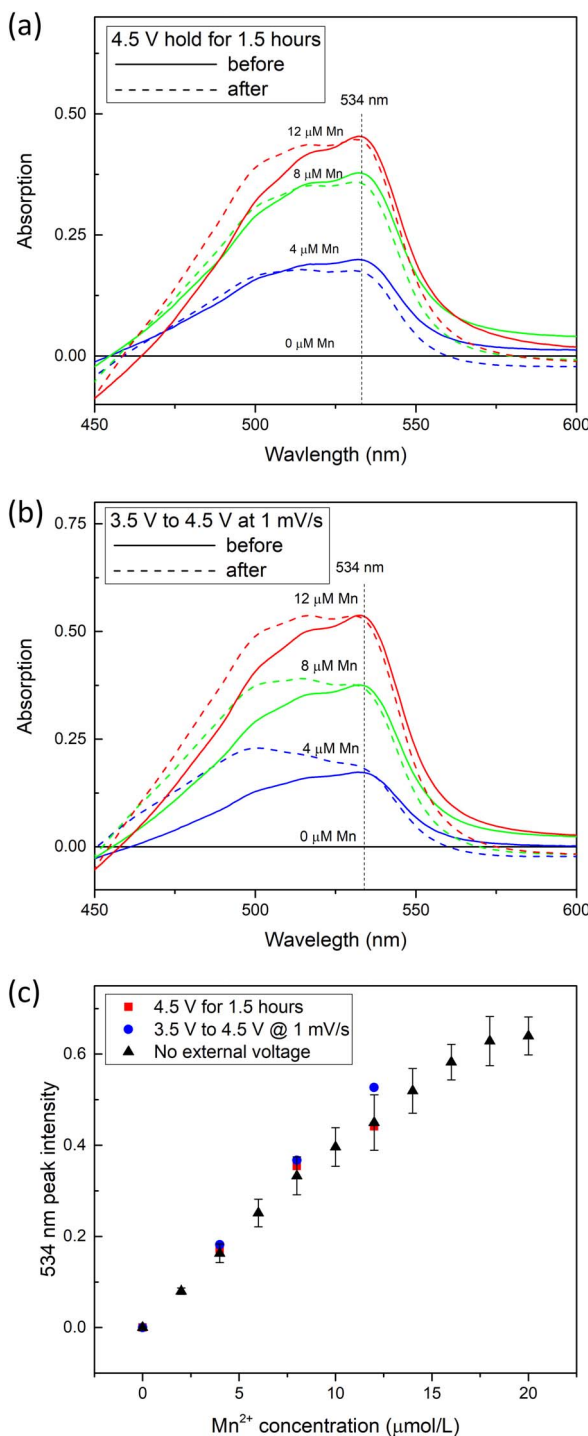


Figure 3. Electrochemical stability of the UV-vis probe in electrolyte. (a) UV-vis spectra before (solid line) and after (dash line) applying 4.5 V for 1.5 hours. (b) UV-vis spectra before (solid line) and after (dash line) cyclic voltammetry between 3.5 V and 4.5 V at 1 mV/s for 2 cycles. (c) Characteristic peak intensity at 534 nm before and after applying various electrochemical potentials as a function of Mn²⁺ ion concentration.

at different concentration were introduced to the electrolyte containing PAR and PS. The typical operation conditions for commercial LMO electrodes are between 3.5 V and 4.5 V vs. Li/Li⁺.⁹ In one set of tests, a constant voltage at 4.5 V was applied for 1.5 hours to simulate exposure to high potential in a battery. In a second set of tests, cyclic voltammetry experiments were carried out between 3.5 V and 4.5 V at scan rate 1 mV/s for 2 cycles. Figures 3a and 3b shows the UV-vis

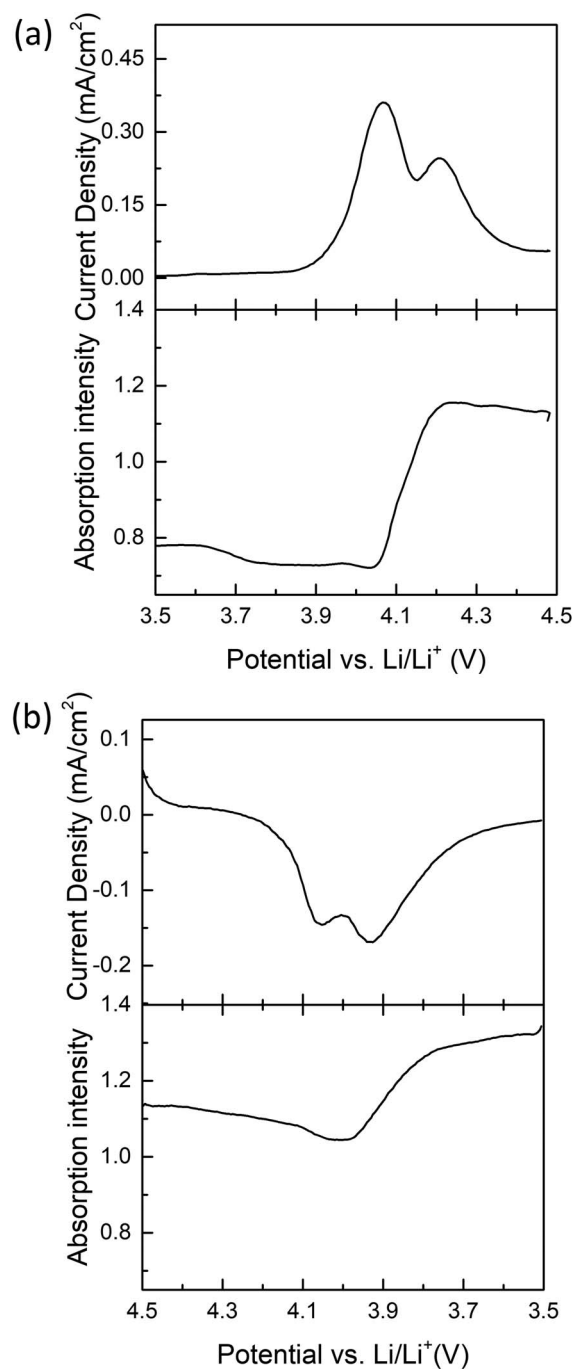


Figure 4. Current response and absorption intensity (at 534 nm peak wavelength) during first cyclic voltammetry test of the custom battery cell designed for in situ detection of Mn dissolution. (a) LMO delithiation process. (b) LMO lithiation process.

spectra and peak intensity extraction for of electrolytes with different Mn²⁺ ion concentrations from potential hold and cyclic voltammetry experiments. In both cases, a slight shift in peak intensity around 500 nm was observed in the spectrum, however, the characteristic peak intensity of PAR-Mn²⁺ complex was consistent regardless of electrochemical conditions at each Mn²⁺ ion concentration. Figure 3c shows the dependence of the characteristic peak intensity on the Mn²⁺ ion concentration in open circuit, constant voltage, and cyclic voltammetry conditions. The results presented in Figure 3 indicate that the external voltage does not affect the chelation of Mn²⁺ ions with PAR. Therefore, UV-vis spectroscopy with the PAR/PS probe is

a promising technique for the in situ detection of Mn²⁺ ions during electrochemical cycling of Li-ion batteries.

The dissolution profile of the LMO cathode during the 1st electrochemical cycle was characterized in the customized cell. Figure 4 shows the current response and change in absorption intensity at 534 nm during cyclic voltammetry. The electrolyte absorption intensity started to increase as the current peak emerged. These results suggest that Mn dissolution is at least partially correlated with electrochemical cycling thereby supporting several well-known dissolution mechanisms^{2,6,7,11} obtained independently via immersion tests. Others have proposed possible Mn dissolution mechanisms such as structural instability of LMO due to phase transition¹⁹ and dissolution assisted by decomposed electrolyte upon cathode delithiation.²⁰ Further research using our in situ UV-vis spectroscopy technique will be carried out to explore and understand the mechanisms of Mn dissolution in LMO to the full extent.

Summary

In the presence of a proton absorber, PAR is demonstrated as a viable UV-vis probe to detect Mn²⁺ ions in Li-ion battery electrolytes. The characteristic peak intensity of the PAR-Mn²⁺ complex was obtained by background subtraction from the raw spectra. A linear relationship between the characteristic peak intensity and Mn²⁺ ion concentration is observed up to a saturation limit of 16 μmol/L for a concentration of 31 μmol/L PAR in the electrolyte. The probe system was stable when subjected to external voltage. The characteristic absorption peak intensity at 534 nm remained unchanged in both potential hold (4.5 V) and cyclic voltammetry (3.5 to 4.5 V at 1 mV/s) experiments. In situ detection of Mn²⁺ ions in electrolyte during cyclic voltammetry was performed in a customized battery cell. Our results reveal the presence of a strong correlation between Mn dissolution and electrochemical cycling.

Acknowledgments

This work was supported by the Center for Electrochemical Energy Science, an Energy Frontier Research Center funded by the U. S.

Department of Energy, Office of Science, Basic Energy Sciences. The authors thank Prof. J. Lyding for the use of the spot-welding machine in battery cell fabrication.

ORCID

L. Zhao  <https://orcid.org/0000-0003-2308-1053>
S. R. White  <https://orcid.org/0000-0002-0831-9097>

References

1. M. M. Thackeray, *J. Am. Ceram. Soc.*, **82**(12), 3347 (1999).
2. D. H. Jang, J. S. Young, and S. M. Oh, *J. Electrochem. Soc.*, **143**(7), 2204 (1996).
3. D. Kim, S. Park, O. B. Chae, J. H. Ryu, Y. U. Kim, R. Z. Yin, and S. M. Oh, *J. Electrochem. Soc.*, **159**(3), A193 (2012).
4. J. Park, J. H. Seo, G. Plett, W. Lu, and A. M. Sastry, *Electrochem. Solid-State Lett.*, **14**(2), A14 (2011).
5. Y. L. Dai, C. Long, and R. E. White, *J. Electrochem. Soc.*, **160**(1), A182 (2013).
6. D. H. Jang and S. M. Oh, *J. Electrochem. Soc.*, **144**(10), 3342 (1997).
7. M. Wohlfahrt-Mehrens, C. Vogler, and J. Garche, *J. Power Sources*, **127**(1), 58 (2004).
8. M. Saulnier, A. Auclair, G. Liang, and S. B. Schougaard, *Solid State Ionics*, **294**, 1 (2016).
9. A. D. Pasquier, A. Blyr, P. Courjal, D. Larcher, G. Amatucci, B. Gerand, and J. M. Tarascon, *J. Electrochem. Soc.*, **146**(2), 428 (1999).
10. J. L. Esbenshade, M. D. Fox, and A. A. Gewirth, *J. Electrochem. Soc.*, **162**(1), A26 (2015).
11. A. Bhandari and J. Bhattacharya, *J. Electrochem. Soc.*, **164**(2), A106 (2017).
12. Y. Terada, Y. Nishiwaki, I. Nakai, and F. Nishikawa, *J. Power Sources*, **97**, 420 (2001).
13. L. F. Wang, C. C. Ou, K. A. Striebel, and J. S. Chen, *J. Electrochem. Soc.*, **150**(7), A905 (2003).
14. C. L. Campion, W. Li, and B. L. Lucht, *J. Electrochem. Soc.*, **152**(12), A2327 (2005).
15. A. Kocyla, A. Pomorski, and A. Kręzela, *J. Inorg. Biochem.*, **152**, 82 (2015).
16. R. W. Alder, P. S. Bowman, W. R. S. Steele, and D. R. Winterman, *Chem. Commun. (London)*, **13**, 723 (1968).
17. E. M. C. Jones, M. N. Silberstein, S. R. White, and N. R. Sottos, *Exp. Mech.*, **54**(6), 971 (2014).
18. E. Ohyoshi, *Polyhedron*, **5**(6), 1165 (1986).
19. W. Choi and A. Manthiram, *J. Electrochem. Soc.*, **153**, A1760 (2006).
20. A. Jarry, S. Gottis, Y. Yu, J. Roque-Rosell, C. Kim, J. Cabana, J. Kerr, and R. Kostecki, *J. Am. Chem. Soc.*, **137**, 3533 (2015).